Document downloaded from:

http://hdl.handle.net/10251/149547

This paper must be cited as:

Benajes, J.; García Martínez, A.; Monsalve-Serrano, J.; Boronat-Colomer, V. (2017). An investigation on the particulate number and size distributions over the whole engine map from an optimized combustion strategy combining RCCI and dual-fuel diesel-gasoline. Energy Conversion and Management. 140:98-108. https://doi.org/10.1016/j.enconman.2017.02.073

The final publication is available at

https://doi.org/10.1016/j.enconman.2017.02.073

Copyright Elsevier

Additional Information

An investigation on the particulate number and size distributions over the whole engine map from an optimized combustion strategy combining RCCI and dual-fuel diesel-gasoline

Energy Conversion and Management, Volume 140, 15 May 2017, Pages 98–108.
http://dx.doi.org/10.1016/j.enconman.2017.02.073

Jesús Benajes, Antonio García*, Javier Monsalve-Serrano and Vicente Boronat

CMT - Motores Térmicos, Universitat Politècnica de València, Camino de Vera s/n, 46022 Valencia, Spain

Corresponding author (*):
Dr. Antonio García (angarma8@mot.upv.es)
Phone: +34 963879659
Fax: +34 963877659

Abstract

Literature demonstrates that, for premixed low temperature combustion concepts, particulate matter cannot be directly extrapolated from soot emissions measurements, as typically done for conventional diesel combustion. This is because the particulate matter from low temperature combustion has low fraction of carbonaceous compounds and great amount of soluble organic fraction, which is not captured by the smoke measurement techniques such as the optical reflectometry. By this reason, the study of the particulate matter characteristics from this combustion techniques requires using specific equipment. The aim of the current work is to gain understanding on the particulate matter characteristics from the dual-mode dual-fuel combustion, which is an optimized combustion strategy that combines fully and highly premixed RCCI regimes at low and medium loads, and switches to dual-fuel diffusion combustion at full load. The study was performed over the whole engine map, using a 15.3:1 compression ratio medium-duty EURO VI diesel engine. In particular, the particulate number and size distributions were sampled using a scanning mobility particle sizer and a condensation particle counter, which allow measuring the size distribution and total number of particles from 5-250 nm. Results demonstrate that the fully premixed RCCI combustion is dominated by small particles (less than 30 nm in mobility diameter), the dual-fuel diffusion mode is dominated by larger particles (around 100 nm in mobility diameter) showing more diesel-like particle size distributions, and the highly premixed reactivity controlled compression ignition regime shows a transitional particle size distribution with two peaks of mobility diameters around 20 and 80 nm.

Keywords

Reactivity controlled compression ignition; dual-fuel combustion; dual-mode; EURO VI emissions; Efficiency; Engine map

1. Introduction

The nitrogen oxides (NOx) and soot emissions limits imposed by the emissions regulations for diesel engines are becoming more and more restrictive over the years, which represents a major concern for researchers and manufacturers [1]. Alternatively to the aftertreatment systems development, the premixed low temperature combustion (LTC) strategies are being extensively studied nowadays as a way to reduce both pollutants directly during the combustion process [2]. These strategies rely on using high rates of exhaust gas recirculation (EGR) and extended fuel-air mixing times as compared to CDC [3], which leads to lower local flame temperatures [4] and avoids fuel-rich zones during the combustion process [5].

The reactivity controlled compression ignition (RCCI) combustion, initially proposed by Inagaki et al. [6] and later developed by Kokjohn et al. [7], has been demonstrated to be more promising than previous LTC strategies such us the homogeneous charge compression ignition (HCCI) [8], diesel partially premixed combustion (PPC) [9], gasoline PPC [10] and gasoline PPC spark assisted [11][12]. The RCCI concept has been extensively studied in different single cylinder engine (SCE) platforms: light- [13], medium- [14] and heavy-duty [15], as well as in multi-cylinder engines [16]. Different strategies have been developed to increase the thermal efficiency of RCCI, such as engine settings optimization: injection settings [17][18], air management conditions [19]; fuel properties modification: fuel variation [20], use of additives [21], use of biofuels [22]; and hardware optimization: piston bowl geometry modification [23], compression ratio optimization [24] or engine cooling reduction [25]. These works have demonstrated that RCCI is able to achieve thermal efficiencies near 50% over a wide range of operating conditions, with NOx emissions under the EURO VI limits and simultaneous ultra-low soot emissions [26]. Nevertheless, a general conclusion form the RCCI literature review is that RCCI operating range is limited to around 8-15 bar IMEP if simultaneous high efficiency, low emissions and low knocking levels are intended [27]. Above this engine load, thermal efficiency or emissions should be compromised at the expense of achieving low pressure rise rates (PRR) [28].

Trying to extend the operation towards higher loads, Benajes et al. [29] developed an optimized dual-mode dual-fuel (DMDF) combustion strategy that combines fully and highly premixed RCCI regimes at low and medium loads, and switches to dual-fuel diffusion combustion at full load. The authors found that this strategy allows to cover the whole engine map with PRR and in-cylinder pressure peaks below 15 bar/CAD and 190 bar, respectively. NOx emissions were below 0.4 g/kWh (EURO VI limit) up to 14 bar IMEP and soot emissions were below 0.8 FSN in the major portion of the engine map, with soot levels equal than or below 0.02 FSN in the region below 7 bar IMEP. In spite of these low soot values, literature demonstrates that, particulate matter (PM) from premixed LTC concepts cannot be directly extrapolated from soot emissions measurements [30], as typically done for CDC [31].

In the past, some researchers have performed studies to characterize the particles emitted during CDC to understand the particle size distribution (PSD) [32] and composition. The different studies agree that PSD for CDC present a bimodal shape, with nucleation (mobility diameter <50 nm) and accumulation mode (diameter >50 nm) particles. In this sense, Kittelson et al. [33] stated that nucleation mode particles might

contain up to the 90% of the number of the particles but less than the 20% of the PM mass emissions. More recently, Storey et al. [34] carried out a speciation about the particles emitted under RCCI operation. The most important results indicate that high boiling range of diesel hydrocarbons was responsible for the PM mass captured on the filter media. Northrop et al. [35] and Glenn et al. [36] demonstrated that RCCI produces lower quantity of particles compared to other LTC strategies. These findings agree with the work performed by Prikhodko et al. [37], which stated that RCCI was highly dominated by nucleation mode particles. These authors also compared the smoke results in terms of filter smoke number (FSN) and PM filter mass measurements. The main conclusions were that RCCI PM is mainly composed of soluble organic fraction (SOF) with almost no elemental carbon [38]. This makes not possible to convert FSN in PM [39], because the smoke meter do not capture the SOF present in the PM of RCCI mode.

The dual-mode dual-fuel (DMDF) combustion concept proposed by Benajes et al. [29] switches between premixed and diffusive combustion strategies to complete the operation over the whole engine map. Thus, considering previous LTC PM findings, a dedicated study is necessary to gain understanding on the PM characteristics from this combustion strategy. In the current research, the particulate number and size distributions from this combustion mode are studied over the whole engine map, using a 15.3:1 compression ratio (CR) medium-duty EURO VI diesel engine. For this purpose, a scanning mobility particle sizer (SMPS), with a condensation particle counter (CDC), has been used to measure the size distribution and total number of particles between 5-250 nm in mobility diameter. Before analyzing the PM results, the main fundamentals of the combustion strategy under investigation is explained to better understand the results extracted from the PM measurements. Later, the smoke emissions and particle number measurements over the whole engine map are presented. Finally the particle size distributions for the different combustion regimes at different loads and speeds, are studied in detail.

2. Materials and methods

2.1. Test cell and engine description

The single-cylinder engine used in this work derives from a state-of-the-art in-line four-cylinder EURO VI diesel engine of 5.1 liters displacement. Their main specifications are shown in Table 1.

Table 1. Engine characteristics.

Style	4 Stroke, 4 valves, DI diesel engine
Manufacturer / model	VOLVO / D5K240
ECU calibration	EURO VI
Maximum power	177 kW @ 2200 rpm
Maximum brake torque	900 Nm @ 1200-1600 rpm
Maximum in-cylinder pressure	190 bar
Bore x Stroke	110 mm x 135 mm
Connecting rod length	212.5 mm
Crank length	67.5 mm
Total displaced volume	5.1 liters
Number of cylinders	4
Compression ratio	15.3:1

Figure 1 shows the test cell layout and the instrumentation used to acquire the data during the engine tests. From the figure, it is seen that the dual-fuel studies are only performed in the first cylinder, while the other three cylinders work under conventional diesel combustion (CDC) governed by the electronic control unit (ECU). For controlling purposes, the in-cylinder pressure signal is measured in the first and fourth cylinder every 0.2 CAD using a Kistler 6125C pressure sensor coupled with a Kistler 5011B10 charge amplifier. This also allows balancing the engine load and pressure peaks between the different cylinders. Finally, it is interesting to note that the dual-fuel combustion process must be studied using indicated values, because all the cylinders share the crankshaft and the dynamometer.

Fully independent intake air, exhaust gas and the EGR lines were used for the dual-fuel cylinder (i.e. first cylinder). A screw compressor was installed at the beginning of the intake line to provide a stable supply of air at a desired pressure and with ambient properties. To condition the intake air before reaching the cylinder, it passes through an air drier and heater. Pressure and temperature of the fresh air are controlled in the intake settling chamber before mixing with the EGR. After that, pressure and temperature are measured in the intake manifold. Later, the charge temperature is measured again after the gasoline injection. In the exhaust line, temperature and pressure are measured in the exhaust manifold as well as in the settling chamber. The next element found is a valve, which is used to reproduce the exhaust backpressure introduced by the turbine in the serial engine. After that, the sample probes from the emissions measurement devices are found. Before the exhaust backpressure, part of the exhaust gases are taken to perform EGR. First of all, the exhaust gas passes through a DPF to eliminate particles from the exhaust stream and the temperature is reduced by means of a water-gas heat exchanger. Due to the temperature drop, some substances can condense, which are trapped in the centrifugal filter. Later, a screw compressor increases the gas pressure to be introduced in the intake manifold and a secondary heat exchanger cools down the gas after the compression. The final temperature of the gas is controlled in the settling chamber, and finally, the EGR rate introduced in the intake manifold is governed by means of a valve just before mixing with the intake air. To determinate the EGR rate introduced, the measured values of intake and exhaust carbon

dioxide (CO_2) concentration with the exhaust emissions analyzer are used. The accuracy of the instrumentation used in the test cell is summarized in Table 2.

Table 2. Accuracy of the instrumentation used in the test cell.

Variable measured	Device	Manufacturer / model	Accuracy
In-cylinder pressure	Piezoelectric transducer	Kistler / 6125C	±1.25 bar
Intake/exhaust pressure	Piezorresistive transducers	Kistler / 4045A10	±25 mbar
Temperature in settling chambers and manifolds	Thermocouple	TC direct / type K	±2.5 °C
Crank angle, engine speed	Encoder	AVL / 364	±0.02 CAD
NOx, CO, HC, O_2, CO_2	Gas analyzer	HORIBA / MEXA-ONE-D1-EGR	4%
FSN	Smoke meter	AVL / 415S	±0.001 FSN
Particles number and size	SMPS	TSI / 3936L75	3.5%
Gasoline/diesel fuel mass flow	Fuel balances	AVL / 733S	±0.2%
Air mass flow	Air flow meter	Elster / RVG G100	±0.1%

The three cylinders working under CDC conditions are also monitored using a similar instrumentation layout than for the cylinder one. This part of the engine has installed the serial components with the exception of the EGR, which was annulled to avoid possible surge conditions in the turbocharger due to the exhaust gas mass flow lost due to the isolation of the first cylinder.

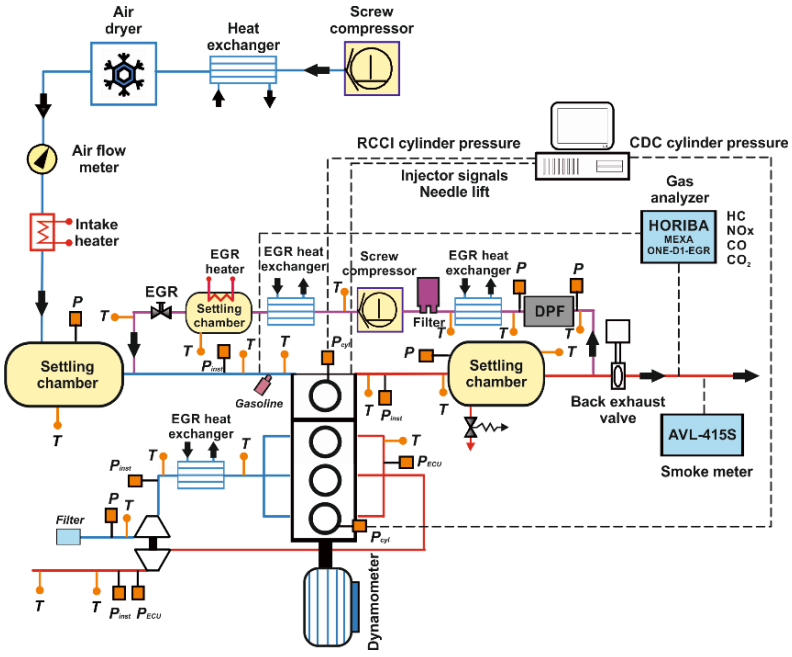

Figure 1. Test cell scheme.

2.2. Fuels and injection systems characteristics

In this study, EN590 diesel and 95 octane number (ON) gasoline are used as high and low reactivity fuels, respectively. The main physical and chemical properties of the fuels,

obtained following American society for testing and materials (ASTM) standards, are depicted in Table 3.

Table 3. Physical and chemical properties of the fuels used.

	Diesel	Gasoline
Density [kg/m^3] (T= 15 °C)	824	720
Viscosity [mm^2/s] (T= 40 °C)	2.8	-
RON [-]	-	95
MON [-]	-	85
Biodiesel content [% by volume]	<0.2	-
Cetane number [-]	51	-
Lower heating value [MJ/kg]	42.92	42.4

The injection systems scheme used to feed the engine with two fuels is shown in Figure 2. A common-rail injection system with a solenoid injector was used to inject the diesel fuel directly into the cylinder. The injector has a 7-hole nozzle and the maximum injection pressure of the system is 2000 bar. On the other hand, a dedicated circuit was developed for the port fuel injection of gasoline. The gasoline injection circuit consists of a fuel pump, fuel tank, fuel filter and a port fuel injector (PFI). The start of gasoline injection timing was fixed 10 CAD after the intake valve opening (IVO) to avoid the fuel pooling on the intake valve seats. The ratio between the two injected fuels is defined as gasoline fraction (GF), which represents the gasoline percentage over the total fuel amount injected. Both injection systems were governed using an in-house developed LabVIEW control system implemented on Drivven hardware. The details of both injection systems are provided in Table 4.

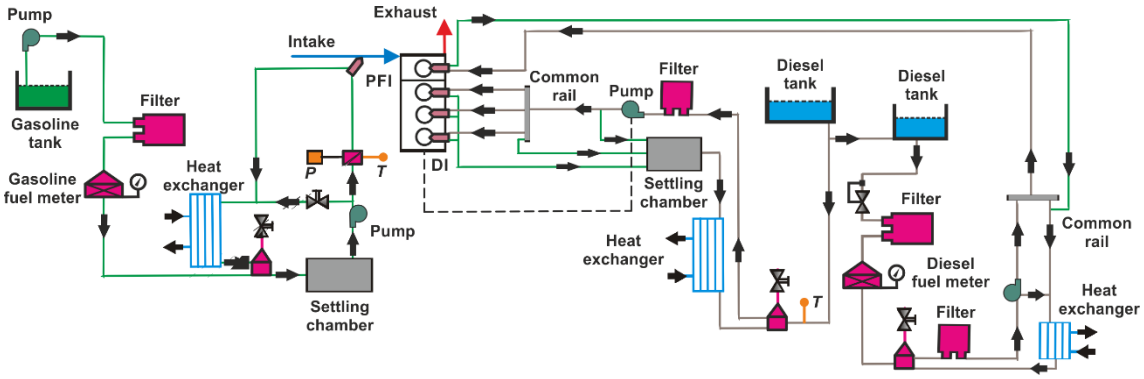

Figure 2. Fuel injection systems scheme.

Table 4. Details of the diesel and gasoline injection systems.

Diesel injector		Gasoline injector	
Actuation Type	Solenoid	Injector Style	Saturated
Steady flow rate @ 100 bar [cm^3/min]	1300	Steady flow rate @ 3 bar [cm^3/min]	980
Included Spray Angle [°]	150	Included Spray Angle [°]	30
Number of Holes	7	Injection Strategy	single
Hole diameter [µm]	177	Start of Injection [CAD ATDC]	340
Maximum injection pressure [bar]	2000	Maximum injection pressure [bar]	5.5

2.3. Smoke and particulate matter sampling systems

The soot content of the exhaust gas was measured with an AVL 415S smoke meter [40]. In this filter-type smoke meter, a defined quantity of exhaust gas passes through a clean filter paper. In particular, three samples of a 1 liter volume each, with paper-saving mode off, were collected for each engine test recorded. Later, the smoke meter utilizes an optical reflectometer to determine the amount of blackening of filter paper by the soot contained in the exhaust gas volume. The blackening on the filter paper is detected by a photoelectric measuring head and translated to FSN (Filter Smoke Number) units on a scale from 0 (filter without blackening) to 10 (filter completely blacked). The detection limit of this device is 0.002 FSN and the resolution is 0.001 FSN.

Particulate matter (PM) from conventional diesel combustion is mainly composed of elemental carbon (i.e. black carbon). By this reason, the soot measurements (in FSN) performed during CDC studies are typically used to estimate the PM concentration (mg/m^3) through the correlation proposed by Christian et al. [31] (Equation 1). This estimation is generally accepted for conventional diesel combustion due to the PM composition. However, since the smoke meter relies on an optical measurement, it may not accurately account for condensable organics in the particulate matter (PM), and hence may underestimate gravimetric PM measurements.

$$\text{Soot}\,[\text{mg/m}^3] = \frac{1}{0.405} \cdot 4.95 \cdot \text{FSN} \cdot \text{e}^{0.38 \cdot \text{FSN}} \quad (1)$$

In this study, the particulate number and size distributions were obtained using a diluter, a scanning mobility particle sizer (SMPS) and a condensation particle counter (CPC), as shown in Figure 3. The sample probe was placed after the exhaust backpressure valve, which is located just after taking the exhaust gas to perform EGR. Firstly, the gas sample is diluted at a ratio of 90:1 using a TSI Rotating Disk thermodiluter to adapt the inlet concentration of the particles to the SMPS requirements. For this purpose, the measurement units are composed of two disks with various cavities. Thus, a raw portion of the exhaust gas is captured when cavities are aligned during the rotatory movement and is driven towards the mixer. In the mixer, the exhaust gas sample dilutes with particle-free air. Then, the diluted sample was heated up to 150 °C to avoid the condensation of the volatiles. The SMPS used is a TSI model 3936L75 system, formed by the Differential Mobility Analyzer (DMA, TSI model 3081) and the Condensation Particle Counter (CPC, TSI model 3775). The DMA measures the particle sizes making them to cross an electric field and the CPC counts the number of particles of mobility diameters between 5-250 nm through a condensation process. The measurement uncertainty of this device is 3.5%. Finally, the data acquisition and PSD processing was done using the Aerosol Instrument Manager software (AIM, TSI).

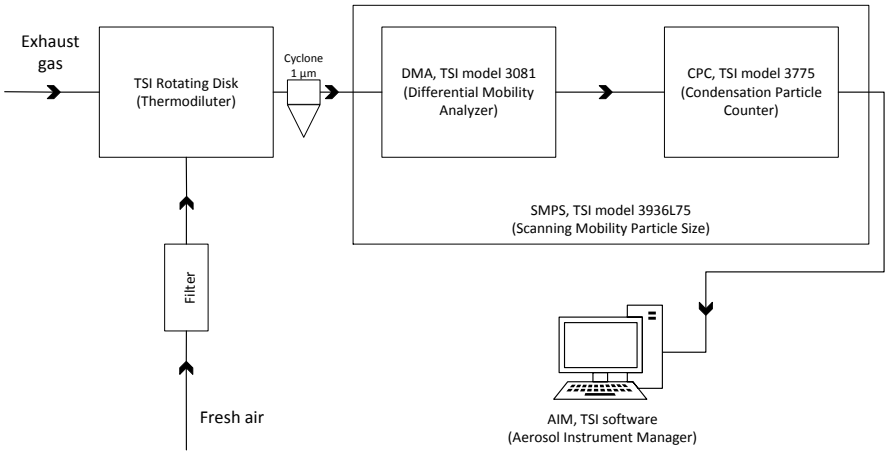

Figure 3. Scanning mobility particle sizer system scheme.

2.4. In-cylinder pressure signal processing

The combustion process analysis was performed using an in-house zero-dimensional model called CALMEC [41]. An ensemble-averaged individual pressure data from 150 consecutive engine cycles, along with the mean variables collected during the engine tests, was used to perform the combustion analysis. Before being averaged, the individual pressure data of each engine cycle was smoothed using a Fourier series low-pass filter. The analysis performed with CALMEC is based on applying the first law of thermodynamics between IVC and EVO for open systems. This is necessary to consider the blow-by phenomenon and the fuel injection process. The mean gas temperature in the cylinder is obtained through the ideal gas equation of state. Moreover, the thermodynamic conditions of the in-cylinder gas necessary to feed the heat transfer models [42] (convection and radiation) are obtained from the in-cylinder pressure signal. Wall temperatures are calculated by means of a lumped conductance model, which is connected to the heat transfer models. Finally, dedicated filling and emptying models were embedded into the zero-dimensional model to provide the fluid-dynamic conditions in the intake and exhaust ports, and therefore the heat transfer in these elements.

The Rate of Heat Release (RoHR) was obtained through the pressure signal processing. The details of the RoHR calculation are fully described in [43]. Also, the bulk gas temperature and the maximum pressure gradient for the different tests were obtained from CALMEC. During the data processing, some other parameters derived from the RoHR were used, such as the start of combustion (SOC) and the combustion phasing, defined as the crank angle degree in which the 10% and 50% of the cumulated heat release is reached, respectively.

3. Results and discussion

This section explains the main results of this research. The first subsection explains the bases of the combustion concept under investigation. The second subsection analyzes the smoke emissions and particle number measurements. Finally, the third subsection shows the particulate size distribution analysis.

3.1. Optimized dual-mode dual-fuel combustion process

The dual-fuel combustion strategy developed to cover the whole engine map switches between RCCI and dual-fuel combustion regimes depending on the engine load. The aim of this combustion strategy is to minimize NOx and soot emissions simultaneously, keeping high brake thermal efficiency, and without exceeding some mechanical constraints defined by the engine manufacturer (PRR <15 bar/CAD and P_{max} <190 bar). The switch between combustion regimes is governed by the diesel injection strategy used, while gasoline injection timing is fixed 10 CAD after the intake valve opening (IVO) in all cases.

From 10% up to 40% load, a fully premixed RCCI strategy is promoted by injecting two diesel pulses in the early compression stroke (between -60 and -40 CAD ATDC). In this way, a greatly extended diesel mixing time can be achieved (from 20 to 40 CAD). As literature demonstrates, this type of RCCI combustion provides near zero soot emissions (i.e., near zero elemental carbon in the particulate matter) with ultra-low NOx emissions, while maintaining or improving brake thermal efficiency versus CDC depending on the operating conditions. However, HC and CO emissions from RCCI are substantially higher than for CDC, mainly in the low load portion of the engine map, where HC and CO values from RCCI are an order of magnitude greater than for CDC. The main limitation found with the fully premixed RCCI combustion regime are the excessive pressure rise rates as engine load increases. This occurs because the in-cylinder charge, composed of homogeneously mixed gasoline and highly premixed diesel, autoignites abruptly as thermodynamic conditions become more favorable. To minimize this problem, from 40% to 75% load, the combustion strategy is switched from fully to highly premixed RCCI. To do this, the second diesel injection is sifted towards the TDC, while the first injection is maintained greatly advanced. This strategy reduces the diesel mixing time as compared to the fully premixed strategy, showing mixing times near 0 CAD, or even negative values in some cases. The first injection timing is kept advanced enough to enhance the spatial stratification of the reactivity towards the squish and crevices, thus improving the gasoline burning in these regions. Under this combustion regime, NOx emissions are maintained below the EURO VI limits, but soot emissions tend to increase due to the mixing time reduction for the second diesel injection. In addition, excessive pressure rise rates also appear for this combustion at around 75% load. By this reason, to cover the engine map region from 75% up to 100% load, a diffusive dual-fuel combustion strategy is applied. This is carried out by setting a single diesel injection near or even after TDC. Thus, by delaying the major part of the combustion event, this combustion regime allows avoiding the excessive pressure rise rates appearing with fully and highly premixed RCCI. However, since the combustion process tends to be more diesel-like, NOx and soot emissions are higher than with RCCI, while HC and CO emissions decrease. The EGR strategy followed to cover the whole engine map is shown in figure 4. As can be seen, up to around 8 bar IMEP, the engine map was covered with only 20% of EGR rate. This is because the fully premixed RCCI strategy allows reaching very low NOx and soot emissions, inherently. When switching to a highly premixed strategy, the EGR rate was increased up to a maximum value of 50% at 12 bar IMEP to extend the premixing time and avoid (or minimize) the diffusion burning of the second diesel injection. Finally, in the upper portion of the map, the EGR rate was reduced again

up to values of around 30% to avoid the excessive soot emissions provoked by the diffusive dual-fuel combustion strategy.

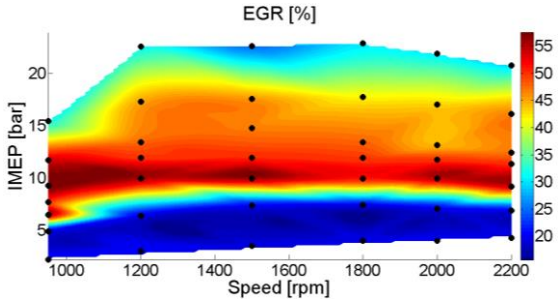

Figure 4. EGR strategy used in the dual-mode dual-fuel combustion strategy.

Figure 5 illustrates the changes in the combustion development depending on the injection strategy implemented, for which the rate of heat release (RoHR) profiles at different engine loads are shown. Also, the boundary conditions and main combustion parameters for these cases are depicted in Table 5. For the sake of brevity, the results are explained using a representative engine speed of 1500 rpm, and the findings for a given load can be extended to the rest of engine speeds. Note that the start of diesel injection timings are marked with symbols in each subfigure. According to the previous explanation, 10% and 25% load cases correspond to a fully premixed RCCI regime (early double diesel injection), 50% load represents the highly premixed RCCI strategy case (separated double diesel injection), and finally, 75% and 100% load show the diffusive dual-fuel strategy (single diesel injection).

Focusing on the RCCI cases, it is seen that the RoHR becomes sharper as load increases. In this sense, the first RoHR peak (where part of diesel fuel and a minimum gasoline quantity is burned) reduces, and the second RoHR peak (where the majority of the gasoline is burned) increases. Thus, the heat release shape evolves from a Weibull-like at 10% load to Gaussian-shaped heat release at 50% load. The reduction of the first RoHR peak from 10% to 25% load is explained by the gasoline fraction (GF) increase, since less diesel is expected to react due to both the less amount of diesel injected and the more reduced global reactivity. Between 10% and 50% load, the reduction of the first RoHR peak occurs because at 50% load the second injection takes place after these first reactions. On the other hand, the second RoHR peak increases as load increases due to the more favorable thermodynamic conditions to burn the low reactivity in-cylinder regions. The RoHR profiles for the dual-fuel diffusion cases (75% and 100% load) have a double-staged shape, with higher RoHR peak in the first combustion phase. The magnitude of each combustion stage varies depending on the engine load. Analyzing the 100% load subfigure, it is seen that the first RoHR peak occurs before the diesel fuel is injected, which confirms that part of the homogeneously mixed gasoline autoignites due to the in-cylinder conditions and not because of the diesel fuel burning reactions. As can be seen, the gasoline autoignition peak is higher for 75% load due to the higher GF used, which promotes very high knocking levels. Thus, to avoid this phenomenon, the GF at 100% load is reduced as compared to 75% load.

Table 5. Boundary conditions and main combustion parameters for the cases at different engine load and 1500 rpm.

Engine speed [rpm]	IMEP [bar]	CA10 [CAD]	CA50 [CAD]	GIE [%]	Comb. Eff. [%]	GF [%]	Eq. ratio [-]	EGR [%]
1500	3.0	-9.5	-2.1	42.5	81.1	60	0.22	20.8
	6.4	-5.7	1.1	44.9	91.4	89	0.32	19.7
	11.9	-4.9	1.5	44.8	97.0	62	0.83	50.2
	17.3	-1.1	9.5	45.1	96.9	45	0.79	45.1
	22.6	-4.1	12.7	47.3	98.1	32	0.81	31.0

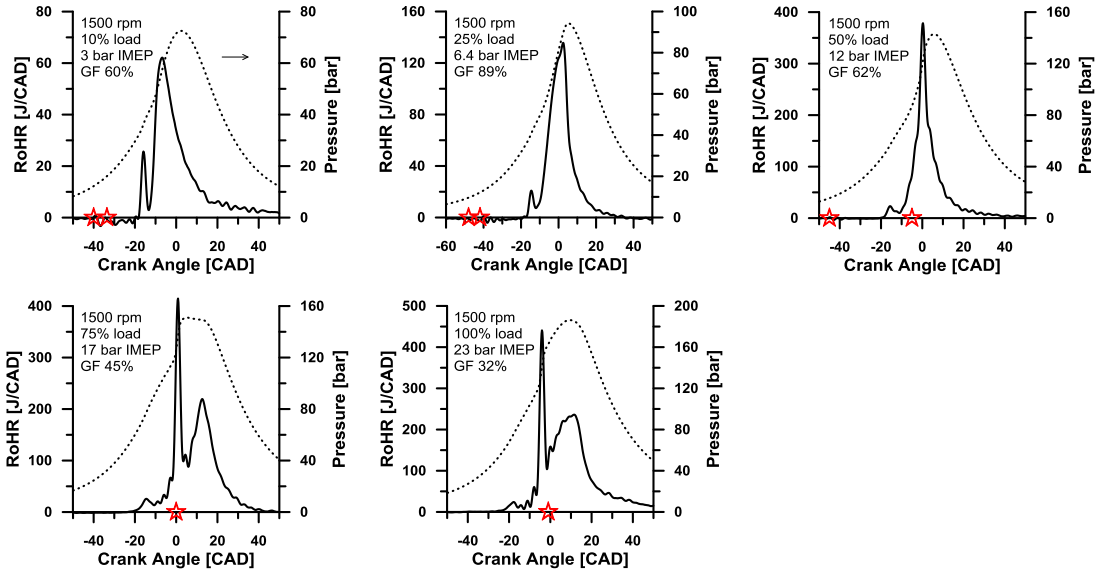

Figure 5. RoHR and pressure traces for different engine loads at 1500 rpm. The start of diesel injection timings are marked with symbols.

To further analyze the gasoline autoignition phenomenon at full load conditions, Figure 6 shows the RoHR profiles at 100% load for the different engine speeds. Their main engine settings and combustion parameters are shown in Table 6. The diesel injection timing for each case is represented with symbols, which is advanced as engine speed increases to maintain similar combustion phasing (CA50) between tests. As it can be seen, from 950 to 1500 rpm, the gasoline autoignites before the diesel fuel is injected in the cylinder. This leads to higher first RoHR peaks versus the other cases (1800 to 2200 rpm). Analyzing the crank angle in which the first RoHR peak appears, it is possible to state that as diesel injection timing is advanced, the RoHR peak is delayed. This is not expected, since diesel fuel should increase the in-cylinder reactivity, and therefore promote early autoignition timing. Considering this, the reason of the first RoHR peak delay should be the engine speed increase, which results in less time for the premixed gasoline to autoignite. This provokes burning less amount of gasoline in this phase, showing lower RoHR peak as diesel injection timing is advanced. The second RoHR peak, mainly driven by the diffusive burning of diesel fuel with part of gasoline, increases as the diesel injection timing is delayed. This occurs because less diesel amount is combusted during the first combustion stage, and therefore is available to be burned in the second phase.

Table 6. Boundary conditions and main combustion parameters for the cases at different engine speed and 100% load.

Engine speed [rpm]	IMEP [bar]	CA10 [CAD]	CA50 [CAD]	GIE [%]	Comb. Eff. [%]	GF [%]	Eq. ratio [-]	EGR [%]
950	15.4	-5.1	15.3	42.3	96.6	40	0.58	31.6
1200	22.6	-4.1	12.7	47.3	98.1	34	0.81	31.0
1500	23.0	-2.9	12.7	46.5	98.0	32	0.76	24.9
1800	23.0	-1.5	13.7	54.2	97.8	34	0.67	30.2
2000	21.9	-0.5	12.1	50.0	97.6	34	0.72	30.3
2200	20.8	0.7	12.9	44.6	97.4	29	0.72	29.7

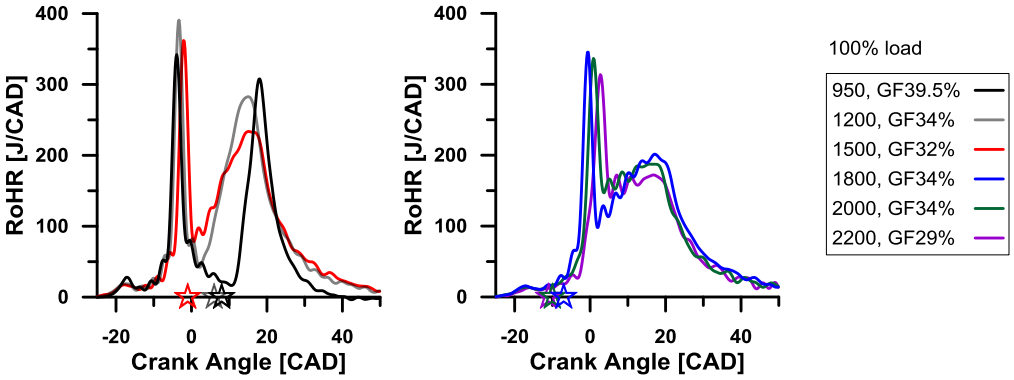

Figure 6. RoHR for the different engine speeds at 100% load. The start of diesel injection timings are marked with symbols.

3.2. Smoke emissions and particle number measurements

Figure 7 shows the smoke emissions and total particle number maps for the dual-mode dual-fuel combustion strategy described in the previous section. Comparing qualitatively both subfigures, it is seen that the maps present greater similarities in the load region above 14 bar IMEP, where the diffusive dual-fuel strategy is applied. The higher FSN values in this region suggest that particulates tend to be more diesel-like as load increases, i.e. mainly composed of elemental carbon. This thought is reinforced by the high coherence between the smoke meter and condensation particle counter (CPC) measurements. By contrast, less similarities between both maps are found in the region below 14 bar IMEP, where fully and highly premixed RCCI strategies are implemented. In this region, FSN cannot be related to the particulates measurement, since they are expect not to be of carbonaceous nature, but be mainly composed of semi-volatile hydrocarbon species, as can be inferred from figure 8.

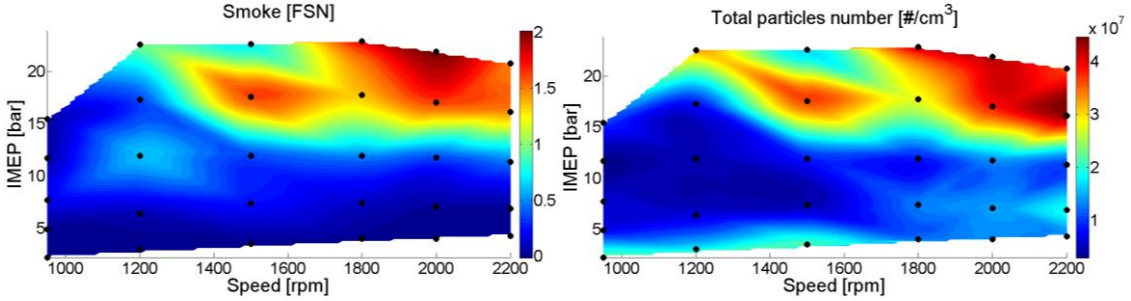

Figure 7. Smoke emissions and total particles number for the dual-mode dual-fuel combustion strategy.

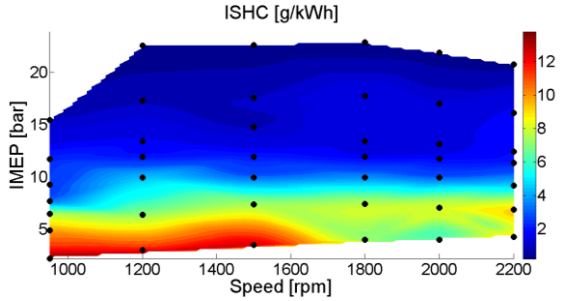

Figure 8. Hydrocarbon emissions map for the dual-mode dual-fuel combustion strategy.

Figure 9 shows the total particle number in the accumulation mode (mobility diameter <30 nm) and nucleation mode (from 30 to 250 nm). Nucleation mode particles are primary composed of condensed hydrocarbon species, whose appearance is favored by the low temperature combustion process [44]. By contrast, accumulation mode particles contain elemental carbon species (i.e., soot particles) similar to those found during conventional diesel combustion [45], and act as a sink for volatile species [46]. Considering this, the Figure 9 allows to identify in a first approach the nature of the particles for each combustion mode. From the figure, it is seen that nucleation mode particles are dominant for the fully and highly premixed RCCI combustion mode, while accumulation mode particles are entirely confined in the high load region of the map, corresponding to the dual-fuel diffusion strategy. Prikhodko et al. [47] demonstrated that conventional diesel oxidation catalysts are effective to reduce nucleation mode particles by diffusion [48]. In particular, the authors found that 35% of nucleation mode particles from RCCI were effectively removed by the DOC with inlet gas temperatures of around 250 °C. The same authors proved that using a diesel particulate filter (DPF) after the DOC, which is a standard aftertreatment layout for current diesel engines, the particulate conversion efficiency increased to near 99% due to the hydrocarbons absorption by the DPF. By contrast, the nucleation mode particles from RCCI were found to be not reduced by the DOC, as occurs during conventional diesel combustion.

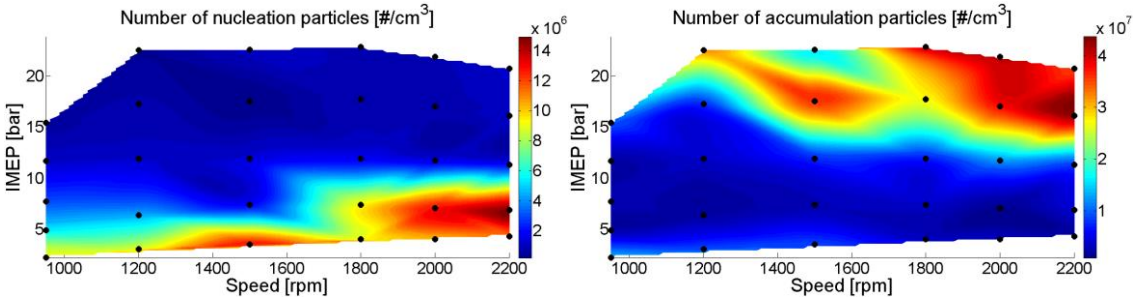

Figure 9. Total number of nucleation (Dp <30 nm) and accumulation (30 <Dp <250 nm) particles for the dual-mode dual-fuel combustion strategy.

To understand the origin of the particulates in each combustion mode, Figure 10 shows the gasoline fraction and diesel mixing time used to cover the whole engine map. The gasoline fraction was typically set to the highest value that could be achieved with an acceptable combustion stability (COV_{IMEP} <5%) and moderate HC emissions. The diesel mixing time is calculated as the interval between the end of the last injection event and the start of combustion (SOC), which has been defined as the crank angle in which the

heat release rate reaches 10% (CA10). As it can be seen, the region above 14 bar IMEP shows mixing times between 0 and -20 CAD, which means the coexistence of the diesel injection and combustion processes during a certain period. This fact, together with the higher rate of diesel to gasoline injected (lower GF), explains the carbonaceous (high FSN) nature of the particulates in this portion of the engine map. By contrast, in the region below 14 bar IMEP, the mixing time values range from 20 to 40 CAD and gasoline fraction ranges from 65% to 95%. The combination of an extended mixing time and low amount of diesel fuel injected allows avoiding fuel-rich zones, and therefore the formation of elemental carbon soot. However, these conditions promote high levels of unburned hydrocarbon species, which are prone to condense under low exhaust temperatures. This leads to an increase of the nucleation mode particles, characterized by a high amount of soluble organic fraction [49].

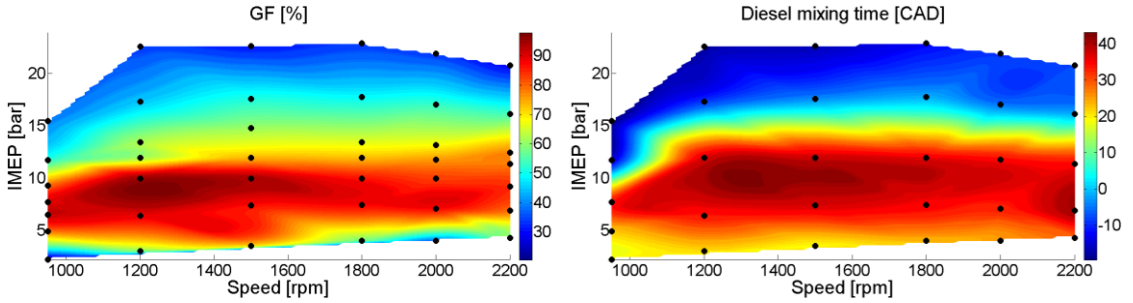

Figure 10. Gasoline fraction and diesel mixing time for the dual-mode dual-fuel combustion strategy.

3.3. Particle size distributions analysis

The classification of the particulate sizes by nucleation or accumulation modes is useful, nevertheless, the analysis of the complete spectra is necessary to gain understanding on the particulate characteristics for the different combustion regimes. For this purpose, Figure 11 shows the effect of the engine load on the particle size distribution (PSD) at different engine speeds, measured with the scanning mobility particle sizer (SMPS). Cases at 10% and 25% correspond to the fully premixed RCCI regime, 50% load case corresponds to the highly premixed RCCI strategy, and 75% and 100% measurements come from the diffusion dual-fuel combustion.

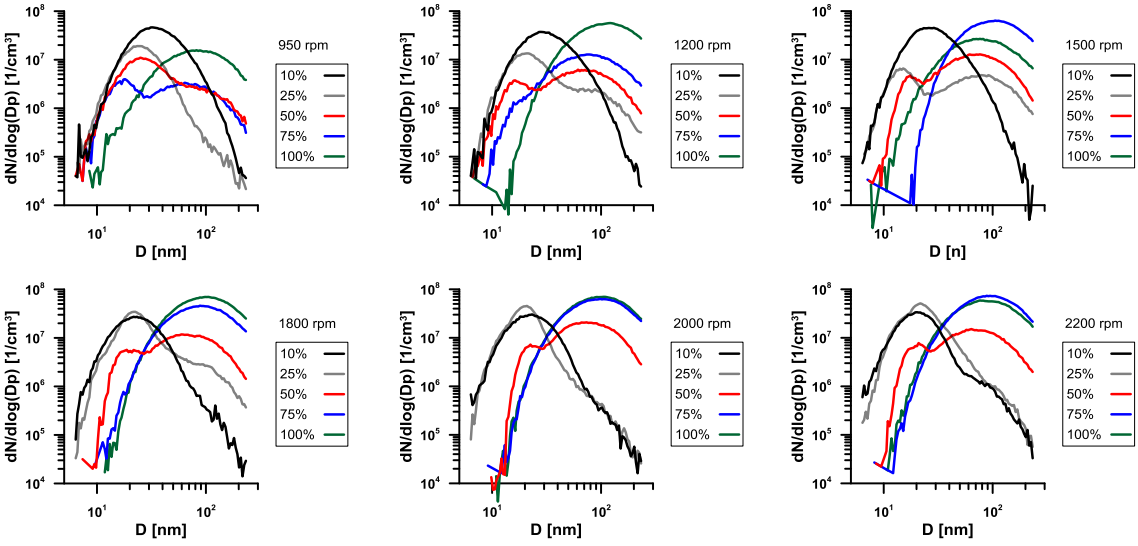

Figure 11. Effect of engine load on particle size distribution at different engine speeds.

Comparing the different subfigures, it is seen that PSDs are mainly dominated by the combustion regime implemented (i.e., engine load), while the engine speed has little impact on them. The results suggest that the fully premixed RCCI combustion is dominated by small particles (mobility diameter peak ≈30 nm), the dual-fuel diffusion mode is dominated by larger particles (mobility diameter peak ≈100 nm) and the highly premixed RCCI regime shows a transitional PSDs, with two peaks of mobility diameter at around 20 and 80 nm. As found in the previous section, the increase of the particles diameter as load increases implies greater soot formation, which results in higher FSN values. This fact can be confirmed looking at Figure 12, which shows the relationship between the smoke measurements in FSN units and the total quantity of bigger particulates, obtained as the integral of the PSD curves for mobility diameters >100 nm. As it can be seen, the FSN measurements and the total quantity of bigger particulates follow the same trend, which means that effectively, these large particles are mainly formed by carbonaceous species (i.e., black carbon soot). In general, the fully premixed RCCI regime shows no bigger particles, while some amount of them can be identify in the highly premixed RCCI strategy. This is coherent with the findings reported by Storey et al. [45], which stated that RCCI particles appear to be composed of a solid carbon core, over which semi-volatile hydrocarbon species tend to condense.

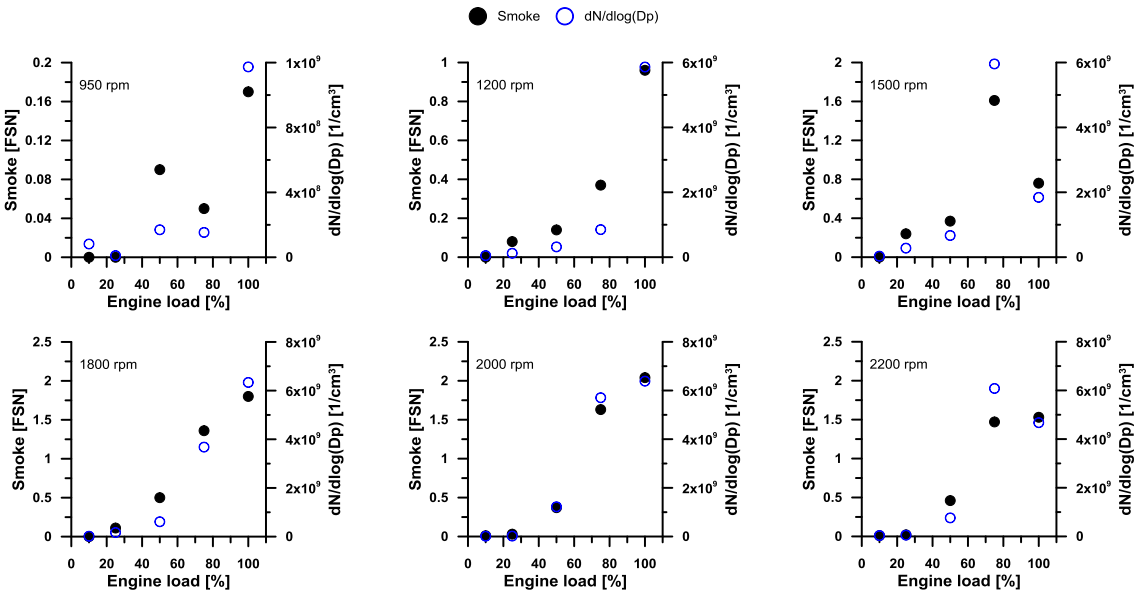

Figure 12. Relationship between the smoke measurements in filter smoke number (FSN) units and total number of bigger particles (mobility diameter >100 nm).

4. Conclusions

The present work studied the particulate number and size distributions from an optimized dual-mode duel-fuel combustion using a scanning mobility particle sizer, which allowed to measure the size distribution of the particles from 5-250 nm. Also, the smoke emissions were measured using a smoke meter. The major findings are summarized as follows:

- Smoke and total particle number maps were found to be similar in the region above 14 bar IMEP. This means that the diffusive dual-fuel strategy leads to large particles of carbonaceous nature (i.e. soot particles), as those from conventional diesel combustion.

- No coherence was found between the smoke and total particles number maps in the low load region. This reveals that particles from the fully and highly premixed RCCI regimes are mainly composed of soluble organic fraction coming from volatile species, which cannot be captured by the smoke meter.
- The particle size distributions (PSD) curves are mainly governed by the engine load (i.e., the combustion regime proposed) and not by the engine speed.
- The fully premixed RCCI combustion is dominated by small particles (diameter ≈30 nm), the dual-fuel diffusion mode is dominated by larger particles (diameter ≈100 nm), and the highly premixed RCCI regime shows a transitional particle size distribution with two peaks of mobility diameters around 20 and 80 nm.
- Some large particles were also found for the RCCI regimes. This finding is coherent with literature, which describes the RCCI particle as a nucleus of carbonaceous nature over which the volatile species tend to condense.

Acknowledgments

This investigation has been funded by VOLVO Group Trucks Technology. The authors also acknowledge the Spanish economy and competitiveness ministry for partially supporting this research (HiReCo TRA2014-58870-R). The predoctoral contract of the author V. Boronat (FPI-S2-2017-2882) is granted by the Programa de Apoyo para la Investigación y Desarrollo (PAID) of the Universitat Politècnica de València. The author J. Monsalve-Serrano acknowledges the financial support from the Universitat Politècnica de València under the Grant “Ayudas Para la Contratación de Doctores para el Acceso al Sistema Español de Ciencia, Tecnología e Innovación”.

References

[1] European Parliament, Council of the European. Regulation (EC) No 595/2009 of the European Parliament and of the Council on type-approval of motor vehicles and engines with respect to emissions from heavy duty vehicles (Euro VI). Official Journal of the European Union 2009, 188, 1-13.

[2] Imtenan S, Varman M, Masjuki H, Kalam M, Sajjad H, Arbab M, Rizwanul Fattah I. Impact of low temperature combustion attaining strategies on diesel engine emissions for diesel and biodiesels: A review. Energy Conversion and Management, Volume 80, April 2014, Pages 329-356.

[3] Splitter D, Wissink M, Hendricks T, Ghandhi J, Reitz R. Comparison of RCCI, HCCI, and CDC Operation from Low to Full Load, THIESEL 2012 Conference on Thermo- and Fluid Dynamic Processes in Direct Injection Engines, 2012.

[4] Neely G, Sasaki S, Huang Y, Leet J, Stewart D. New Diesel Emission Control Strategy to Meet US Tier 2 Emissions Regulations. SAE Technical Paper, 2005-01-1091, 2005.

[5] Garcia A, Monsalve-Serrano J, Heuser B, Jakob M, Kremer F, Pischinger S. Influence of fuel properties on fundamental spray characteristics and soot emissions using different tailor-made fuels from biomass. Energy Conversion and Management, Volume 108, 15 January 2016, Pages 243-254.

[6] Inagaki K, Fuyuto T, Nishikawa K, Nakakita K, Sakata I. Dual-fuel PCI combustion controlled by in-cylinder stratification of ignitability. SAE technical paper 2006-01-0028; 2006.

[7] Kokjohn S, Hanson R, Splitter D, Reitz R. Fuel reactivity controlled compression ignition (RCCI): a pathway to controlled high-efficiency clean combustion, International Journal of Engine Research, 2011. Volume 12, June 2011, Pages 209-226.
[8] Shi L, Deng K, Cui Y, Qu S, Hu W. Study on knocking combustion in a diesel HCCI engine with fuel injection in negative valve overlap. Fuel, Volume 106, April 2013, Pages 478–483.
[9] Jain A, Singh A, Agarwal A. Effect of fuel injection parameters on combustion stability and emissions of a mineral diesel fueled partially premixed charge compression ignition (PCCI) engine. Applied Energy, Volume 190, 15 March 2017, Pages 658-669.
[10] Leermakers C, Bakker P, Nijssen B, Somers L, Johansson B. Low octane fuel composition effects on the load range capability of partially premixed combustion. Fuel, Volume 135, 1 November 2014, Pages 210-222.
[11] Benajes J, Molina S, García A, Monsalve-Serrano J, Durrett R. Conceptual model description of the double injection strategy applied to the gasoline partially premixed compression ignition combustion concept with spark assistance. Applied Energy, Volume 129, 15 September 2014, Pages 1-9.
[12] Benajes J, Molina S, García A, Monsalve-Serrano J, Durrett R. Performance and engine-out emissions evaluation of the double injection strategy applied to the gasoline partially premixed compression ignition spark assisted combustion concept. Applied Energy, Volume 134, 1 December 2014, Pages 90-101.
[13] Qian Y, Wang X, Zhu L, Lu X. Experimental studies on combustion and emissions of RCCI (reactivity controlled compression ignition) with gasoline/n-heptane and ethanol/n-heptane as fuels. Energy, Volume 88, August 2015, Pages 584-594.
[14] Benajes J, García A, Monsalve-Serrano J, Balloul I, Pradel G. Evaluating the reactivity controlled compression ignition operating range limits in a high-compression ratio medium-duty diesel engine fueled with biodiesel and ethanol. International Journal of Engine Research, Volume 18 (1-2), Pages 66-80, 2017.
[15] Desantes JM, Benajes J, García A, Monsalve-Serrano J. The Role of the In-Cylinder Gas Temperature and Oxygen Concentration over Low Load RCCI Combustion Efficiency. Energy, Volume 78, 15 December 2014, Pages 854-868.
[16] Hanson R, Reitz R. Transient RCCI Operation in a Light-Duty Multi-Cylinder Engine. SAE Int. J. Engines 6(3):2013, doi:10.4271/2013-24-0050.
[17] Nazemi M, Shahbakhti M. Modeling and analysis of fuel injection parameters for combustion and performance of an RCCI engine. Applied Energy, Vol. 165, pp 135-150, 2016.
[18] Benajes J, Molina S, García A, Monsalve-Serrano J. Effects of Direct injection timing and Blending Ratio on RCCI combustion with different Low Reactivity Fuels. Energy Conversion and Management, Volume 99, 15 July 2015, Pages 193-209.
[19] Benajes J, Molina S, A. García A, Belarte E, Balloul I. Potential Of Miller Cycle In Reactivity Controlled Compression Ignition Combustion. SIA Powertrain International Conference - The clean compression ignition engine of the future, 21/05/2014, Rouen.
[20] Benajes J, Molina S, García A, Monsalve-Serrano J. Effects of low reactivity fuel characteristics and blending ratio on low load RCCI (reactivity controlled compression ignition) performance and emissions in a heavy-duty diesel engine. Energy, Volume 90, October 2015, Pages 1261–1271.

[21] Dempsey A, Walker N, Reitz R. Effect of Cetane Improvers on Gasoline, Ethanol, and Methanol Reactivity and the Implications for RCCI Combustion. SAE International Journal of Fuels and Lubricants, Vol. 6 no 1, pp. 170-187, 2013.
[22] Yu S, Zheng M. Ethanol–diesel premixed charge compression ignition to achieve clean combustion under high loads. Proceedings of the Institution of Mechanical Engineers, Part D: Journal of Automobile Engineering, 2015. doi: 10.1177/0954407015589870.
[23] Benajes J, García A, Pastor JM, Monsalve-Serrano J. Effects of piston bowl geometry on Reactivity Controlled Compression Ignition heat transfer and combustion losses at different engine loads. Energy, Volume 98, March 2016, Pages 64-77.
[24] Benajes J, Pastor JV, García A, Boronat V. A RCCI operational limits assessment in a medium duty compression ignition engine using an adapted compression ratio. Energy Conversion and Management, Volume 126, 2016, Pages 497-508.
[25] Splitter D, Wissink M, DelVescovo D, Reitz R. RCCI Engine Operation Towards 60% Thermal Efficiency. SAE Technical Paper 2013-01-0279, 2013, doi:10.4271/2013-01-0279.
[26] Benajes J, Pastor JV, García A, Monsalve-Serrano J. The potential of RCCI concept to meet EURO VI NOx limitation and ultra-low soot emissions in a heavy-duty engine over the whole engine map. Fuel, Volume 159, November 2015, Pages 952–961.
[27] Benajes J, García A, Monsalve-Serrano J, Balloul I, Pradel G. An assessment of the dual-mode reactivity controlled compression ignition/conventional diesel combustion capabilities in a EURO VI medium-duty diesel engine fueled with an intermediate ethanol-gasoline blend and biodiesel. Energy Conversion and Management, Volume 123, July 2016, Pages 381-391.
[28] Benajes J, Pastor JV, García A, Monsalve-Serrano J. An experimental investigation on the Influence of piston bowl geometry on RCCI performance and emissions in a heavy-duty engine. Energy Conversion and Management, Volume 103, October 2015, Pages 1019-1030.
[29] J. Benajes, A. García, J. Monsalve-Serrano, V. Boronat, Achieving clean and efficient engine operation up to full load by combining optimized RCCI and dual-fuel diesel-gasoline combustion strategies. Energy Conversion and Management, Volume 136, 15 March 2017, Pages 142-151.
[30] Dempsey A, Curran S, Storey J, Eibl M, Pihl J, Prikhodko V, Wagner R, Parks J. Particulate Matter Characterization of Reactivity Controlled Compression Ignition (RCCI) on a Light Duty Engine. SAE Technical Paper 2014-01-1596, 2014, doi:10.4271/2014-01-1596.
[31] Christian R, Knopf F, Jasmek A, Schindler W. A new method for the filter smoke number measurement with improved sensitivity. MTZ Motortechnische Zeitschift, Vol. 54, pp. 16-22, 1993.
[32] Shi J, Harrison R, Brear F. Particle size distribution from a modern heavy duty diesel engine. The Science of the Total Environment, 1999-235-305, 1999.
[33] Kittelson D. Engine and Nanoparticles: a Review. Journal of Aerosol Science, 1998-29-575, 1998.
[34] Storey J, Curran S, Lewis S, Barone T, Dempsey T, Moses-DeBusk M, Hanson M, Prikhodko V, Northrop W. Evolution and current understanding of physicochemical characterization of particulate matter from reactivity controlled compression

ignition combustion on a multi cylinder light-duty engine. International Journal of Engine Research, 2016.
[35] Northrop, William F., Praveen V. Madathil, Stanislav V. Bohac, and Dennis N. Assanis. 2011. Condensational Growth of Particulate Matter from Partially Premixed Low Temperature Combustion of Biodiesel in a Compression Ignition Engine. Aerosol Science and Technology 45 (1): 26-36.
[36] Lucachick, Glenn, Scott Curran, John Storey, Vitaly Prikhodko, and William F. Northrop. 2016. Volatility Characterization of Nanoparticles from Single and Dual-Fuel Low Temperature Combustion in Compression Ignition Engines. Aerosol Science and Technology 50 (5): 436-47.
[37] Prikhodko V, Curran S, Barone T, Lewis S. Emission Characteristics of a Diesel Engine Operating with In-Cylinder Gasoline and Diesel Fuel Blending. SAE Int. J. Fuels Lubr., 2010-946, 2010.
[38] Zhang, Y, Ghandhi J, Rothamer D. Comparison of Particulate Size Distributions from Advanced and Conventional Combustion - Part I: CDC, HCCI, and RCCI. SAE Int. J. Engines 7(2):820-834, 2014, doi:10.4271/2014-01-1296.
[39] Northrop W, Bohac S, Chin J, Assanis D. Comparison of filter smoke number and elemental carbon mass from partially premixed low temperature combustion in a direct-injection diesel engine. J Eng Gas Turb Power 2011-133, 2011.
[40] AVL. Smoke value measurement with the filter-paper-method (Application notes), June2005, www.avl.com/documents/10138/885893/Application+Notes
[41] Payri F, Olmeda P, Martín J, García A. A complete 0D thermodynamic predictive model for direct injection diesel engines. Applied Energy, Volume 88, Issue 12, December 2011, Pages 4632-4641.
[42] Payri F, Olmeda P, Martin J, Carreño R. A New Tool to Perform Global Energy Balances in DI Diesel Engines. SAE Int. J. Engines 7(1):2014, doi:10.4271/2014-01-0665.
[43] Benajes J, García A, Monsalve-Serrano J, Boronat V. Dual-Fuel Combustion for Future Clean and Efficient Compression Ignition Engines. Applied Sciences 7(1):36, 2017.
[44] Prikhodko V, Curran S, Barone T, Lewis S, Storey J, Cho K, et al. Emission characteristics of a diesel engine operating with in-cylinder gasoline and diesel fuel blending. SAE Int J Fuels Lubr 2010; 3: 946–955.
[45] Storey J, Curran S, Lewis S, Barone T, Dempsey A, Moses-DeBusk M, Hanson R, Prikhodko V, Northrop W. Evolution and current understanding of physicochemical characterization of particulate matter from reactivity controlled compression ignition combustion on a multicylinder light-duty engine. International Journal of Engine Research, 1-15, 2016.
[46] Abdul-Khalek I, Kittelson D, Brear F. Diesel Trap Performance: Particle Size Measurements and Trends. SAE Technical Paper 982599, 1998, doi:10.4271/982599.
[47] Prikhodko V, Curran S, Barone T, Lewis S, Storey J, Cho K, Wagner R, Parks J. Diesel oxidation catalyst control of hydrocarbon aerosols from reactivity controlled compression ignition combustion. In: Proceedings of the ASME 2011 international mechanical engineering congress and exposition (vol. 9), Denver, CO, 11–17 November 2011, pp.273– 278. New York: ASME.
[48] Konstandopoulos A, Kostoglou M, Skaperdas E, Papaioannou E, Zarvalis D, Kladopoulou E. Fundamental Studies of Diesel Particulate Filters: Transient Loading,

Regeneration and Aging. SAE Technical Paper 2000-01-1016, doi:10.4271/2000-01-1016.

[49] Jiang H, Wang J, Shuai S. Visualization and performance analysis of gasoline homogeneous charge induced ignition by diesel. SAE technical paper 2005-01-0136, 2005.

Abbreviations

AIM: Aerosol Instrument Manager

ASTM: American Society of Testing and Materials

ATDC: After Top Dead Center

BDC: Bottom Dead Center

CAD: Crank Angle Degree

CA10: Crank angle of 10% heat release

CA50: Crank angle at 50% heat release

CDC: Conventional Diesel Combustion

CO: Carbon Monoxide

CO_2: Carbon Dioxide

COV: Coefficient of Variation

CPC: Condensation Particle Counter

CR: Compression Ratio

DMA: Differential Mobility Analyzer

DMDF: Dual-mode dual-fuel

DOC: Diesel Oxidation Catalyst

DPF: Diesel Particulate Filter

ECU: Electronic Control Unit

EGR: Exhaust Gas Recirculation

EVO: Exhaust Valve Open

FSN: Filter Smoke Number

GF: Gasoline Fraction

HC: Hydrocarbons

HCCI: Homogeneous Charge Compression Ignition

IMEP: Indicated Mean Effective Pressure

IVC: Intake Valve Close

IVO: Intake Valve Open

LTC: Low Temperature Combustion

MCE: Multi Cylinder Engine

NOx: Nitrogen Oxides

ON: Octane Number

PFI: Port Fuel Injection

PPC: Partially Premixed Charge

PSD: Particle Size Distribution

PRR: Pressure Rise Rate

RCCI: Reactivity Controlled Compression Ignition

RoHR: Rate of Heat Release

SCE: Single Cylinder Engine

SCR: Selective Catalytic Reduction

SMPS: Scanning Mobility Particle Sizer

SOC: Start of Combustion

SOF: Soluble Organic Fraction